Necrostatin-1 [4311-88-0]

NB-64-08656-5mg
NB-64-08656-10mg
NB-64-08656-25mg
NB-64-08656-50mg
NB-64-08656-100mg
NB-64-08656-200mg
NB-64-08656-500mg
NB-64-08656-1mL

Necrostatin-1 [4311-88-0]

#Cat: NB-64-08656-5mg **Size: 5mg**
#Cat: NB-64-08656-10mg **Size: 10mg**
#Cat: NB-64-08656-25mg **Size: 25mg**
#Cat: NB-64-08656-50mg **Size: 50mg**
#Cat: NB-64-08656-100mg **Size: 100mg**
#Cat: NB-64-08656-200mg **Size: 200mg**
#Cat: NB-64-08656-500mg **Size: 500mg**
#Cat: NB-64-08656-1mL **Size: 1mL**

Chemical Properties

CAS No. : 4311-88-0
Formula : C13H13N3OS
Molecular Weight : 259.33
Appearance : Solid
Storage : Powder: -20°C for 3 years | In solvent: -80°C for 1 year

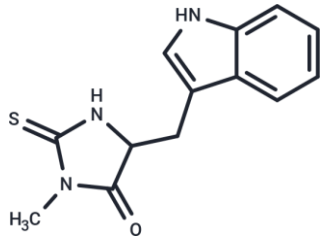

Biological Description

Description	Necrostatin-1 (Nec-1) is a specific RIP1 inhibitor and necrotic apoptosis inhibitor, which inhibits TNF-α-induced necrotic apoptosis and also inhibits IDO.
Targets(IC50)	Ferroptosis, Autophagy, Indoleamine 2,3-Dioxygenase (IDO), RIP kinase
In vitro	**METHODS:** Human hepatocellular carcinoma cells Huh7 and SK-HEP-1 were pretreated with Necrostatin-1 (10-20 μM) for 1 h, and then treated with sulfasalazine, erastin or RSL3 for 24 h. Cell viability was measured by CellTiter Glo® assay. **RESULTS:** Necrostatin-1 significantly blocked the decrease in cell viability induced by sulfasalazine and erastin in both cell lines and partially reversed the decrease in cell viability induced by RSL3 in SK-HEP-1 cells. [1] **METHODS:** Human histiocytic lymphoma cells U937 were treated with Necrostatin-1 (1- 20 μM), zVAD.fmk (100 μM), and TNFα (10 ng/mL) for 72 h. Cell viability was detected by ATP-based viability assay. **RESULTS:** Necrostatin-1 effectively blocked the necrotic death of U937 cells in a concentration-dependent manner. [2] **METHODS:** H/R injury-induced human renal papillomatous cells HK-2 were treated with Necrostatin-1 (30 mmol/L) for 2-12 h. Cell death was analyzed by Flow Cytometry. **RESULTS:** Necrostatin-1 partially protected HK-2 cells from H/R-induced necrosis. [3]
In vivo	**METHODS:** To study the pathophysiology of contrast-induced AKI

	(CIAKI), Necrostatin-1 (1.65 mg/kg) was administered intraperitoneally as a single injection to C57BL/6 mice, and CIAKI was induced by using radiocontrast media (RCM) 15 min later. **RESULTS:** Necrostatin-1 prevented osmotic nephropathy and CIAKI. Necrostatin-1 blocked RCM-induced peritubular capillary dilatation, suggesting that the structural domain of RIP1 kinase has a novel role in regulating the microvascular hemodynamics and pathophysiology of CIAKI that is independent of cell death. [4] **METHODS:** To investigate the protective effect and mechanism of hepatitis in mice, Necrostatin-1 (1.8 mg/kg) was administered intraperitoneally to C57BL/6 mice as a single injection, and concanavalin A was used to induce hepatitis 1 h later. **RESULTS:** Improvements in liver function and histopathologic changes, as well as suppression of inflammatory cytokine production, were observed in Necrostatin-1- injected mice. The expression of TNF-α, IFN-γ, IL2, IL6, and RIP1 was significantly reduced in Necrostatin-1-injected mice, and autophagosome formation was significantly reduced by Necrostatin-1 treatment. The RESULTS suggest that Necrostatin- 1 prevents concanavalin A-induced liver injury through RIP1-related and autophagy- related pathways. [5]
Kinase Assay	The assay was performed essentially as described. 293T cells were transfected with pcDNA3-FLAG-RIP1 vector, vectors encoding RIP1 mutant proteins or pcDNA3-RIP2-Myc and pcDNA3-FLAG-RIP3 vectors using standard Ca3(PO4)2 precipitation procedure. Culture medium was replaced 6 h after the transfection and cells were lysed 48 h later in the TL buffer consisting of 1% Triton X-100, 150 mM NaCl, 20 mM HEPES, pH 7.3, 5 mM EDTA, 5 mM NaF, 0.2 mM NaVO3 and complete protease inhibitor cocktail. Immunoprecipitation was carried out for 16 h at 4 °C using anti-FLAG M2 agarose beads, followed by three washes with TL buffer and two washes with 20 mM HEPES, pH 7.3. Beads were incubated in 15 µl of the reaction buffer containing 20 mM HEPES, pH 7.3, 10 mM MnCl2 and 10 mM MgCl2 for 15 min at 23–25 °C in the presence of different concentrations of necrostatins. For these assays, compound stocks (in DMSO) were diluted to appropriate concentrations in DMSO before the addition to the reactions to maintain final concentration of DMSO for all samples at 3%. Kinase reaction was initiated by addition of 10 µM cold ATP and 1 mCi of [γ-32P] ATP, and reactions were carried out for 30 min at 30 °C. Reactions were stopped by boiling in SDS-PAGE sample buffer and subjected to 8% SDS-PAGE. RIP1 band was visualized by analysis in a Storm 8200 Phosphorimager. Similar protocol was used for endogenous RIP1 kinase reactions, except mouse monoclonal RIP1 antibody and protein magnetic beads or rabbit RIP1 antibody-coupled agarose beads were used. For recombinant baculovirally expressed RIP1, protein was expressed

	in Sf9 cells according to manufacturer's instructions and purified using glutathione-sepharose beads. Protein was eluted in 50 mM Tris-HCl, pH 8.0 supplemented with 10 mM reduced glutathione, and eluted protein was used in the kinase reactions, supplemented with 5 × kinase reaction buffer (100 mM HEPES, pH 7.3, 50 mM MnCl2, 50 mM MgCl2, 50 µM cold ATP and 5 µCi of [γ-32P]ATP) [1].
Cell Research	Determination of EC50 was performed in FADD-deficient Jurkat cells treated with human TNFα as previously described. Briefly, cells were seeded into 96-well plates and treated with a range of necrostatin concentrations (30 nM to 100 µM, 11 dose points) in the presence and absence of 10 ng ml–1 human TNFα for 24 h. For these and all other cellular assays, compound stocks (in DMSO) were diluted to appropriate concentrations in DMSO before addition to the cells to maintain final concentration of DMSO for all samples at 0.5%. Cell viability was determined using CellTiter-Glo luminescent cell viability assay. Ratio of luminescence in compound and TNF-treated wells to compound-treated, TNF-untreated wells was calculated (viability, %) [1].
Animal Research	24 hours after reperfusion, mice received intravenous application of 200 µl PBS or RCM via the tail vein. A single dose of zVAD (10 mg/kg body weight) or Nec-1 (1.65 mg/kg body weight) was applied intraperitoneally 15 min. before RCM-injection. To test the activity of zVAD, we applied zVAD from the same byculture to anti-Fas-treated Jurkat cells to assure its quality before mice were treated with this compound. Mice were harvested another 24 hours after RCM-application (48 hours after reperfusion). Blood samples were obtained from retroorbital bleeding and serum levels of urea and creatinine 5 were determined according to clinical standards in the central laboratory of the University Hospital Schleswig-Holstein, Campus Kiel, Germany, employing an enzymatic ultraviolettest for urea and an enzymatic peroxidase-dependent test for creatinine according to the manufacturer's instructions. Kidneys were conserved for histology. In addition to the demonstrated experiments, we compared the PBS group to mice that only received IRI without 200 µl of PBS and detected no changes in serum concentrations of urea and creatinine or histologically [3].

Solubility Information

Solubility	DMSO: 245 mg/mL (944.74 mM), Sonication is recommended. 10% DMSO+40% PEG300+5% Tween 80+45% Saline: 4 mg/mL (15.42 mM), Solution. (< 1 mg/ml refers to the product slightly soluble or insoluble)

Preparing Stock Solutions

	1mg	5mg	10mg
1 mM	3.8561 mL	19.2805 mL	38.5609 mL
5 mM	0.7712 mL	3.8561 mL	7.7122 mL
10 mM	0.3856 mL	1.928 mL	3.8561 mL
50 mM	0.0771 mL	0.3856 mL	0.7712 mL

Please select the appropriate solvent to prepare the stock solution, according to the solubility of the product in different solvents. Please use it as soon as possible.

Reference

Hanna Y, et al. Necrostatin-1 Prevents Ferroptosis in a RIPK1- and IDO-Independent Manner in Hepatocellular Carcinoma. Antioxidants. 2021 July;10(9):1347.

Hu G, Cui Z, Chen X, et al.Suppressing Mesenchymal Stromal Cell Ferroptosis Via Targeting a Metabolism-Epigenetics Axis Corrects their Poor Retention and Insufficient Healing Benefits in the Injured Liver Milieu.Advanced Science.2023: 2206439.

Yan B, Ai Y, Sun Q, et al. Membrane Damage during Ferroptosis Is Caused by Oxidation of Phospholipids Catalyzed by the Oxidoreductases POR and CYB5R1[J]. Molecular Cell. 2020

Cai H, Qin D, Liu Y, et al.Remodeling of Gut Microbiota by Probiotics Alleviated Heat Stroke-Induced Necroptosis in Male Germ Cells. Molecular Nutrition & Food Research.2023: 2300291.

Zeng H, Xie H, Ma Q, et al.Identification of N-(3-(methyl (3-(orotic amido) propyl) amino) propyl) oleanolamide as a novel topoisomerase I catalytic inhibitor by rational design, molecular dynamics simulation, and biological evaluation. Bioorganic Chemistry.2023: 106734.

Du S, Zeng F, Sun H, et al. Prognostic and therapeutic significance of a novel ferroptosis related signature in colorectal cancer patients. Bioengineered. 2022, 13(2): 2498-2512.

Ning X, Qi H, Yuan Y, et al. Identification of a new small molecule that initiates ferroptosis in cancer cells by inhibiting the system Xc− to deplete GSH. European Journal of Pharmacology. 2022: 175304.

Wang S, Li F, Qiao R, et al. Arginine-Rich Manganese Silicate Nanobubbles as a Ferroptosis-Inducing Agent for Tumor-Targeted Theranostics. ACS nano. 2018 Dec 26;12(12):12380-12392.

Su G, Yang W, Wang S, et al. SIRT1-autophagy axis inhibits excess iron-induced ferroptosis of foam cells and subsequently increases IL-1B and IL-18. Biochemical and Biophysical Research Communications. 2021, 561: 33-39. Wu X, Lu Y, Qin X. Combination of Compound Kushen Injection and cisplatin shows synergistic antitumor activity in p53-R273H/P309S mutant colorectal cancer cells through inducing apoptosis. Journal of Ethnopharmacology.
2021: 114690.

Yao X, Ma S, Peng S, et al. Zwitterionic Polymer Coating of Sulfur Dioxide-Releasing Nanosystem Augments Tumor Accumulation and Treatment Efficacy. Advanced Healthcare Materials. 2020, 9(5): 1901582.

Wang F, Xie M, Chen P, et al. Homoharringtonine combined with cladribine and aclarubicin (HCA) in acute myeloid leukemia: A new regimen of conventional drugs and its mechanism. Oxidative Medicine and Cellular Longevity.
2022

Yang W, Liu S, Li Y, et al. Pyridoxine induces monocyte-macrophages death as specific treatment of acute myeloid leukemia. Cancer Letters. 2020

Li Y, Yang W, Zheng Y, et al. Targeting fatty acid synthase modulates sensitivity of hepatocellular carcinoma to sorafenib via ferroptosis. Journal of Experimental & Clinical Cancer Research.2023, 42(1): 1-19.
Degterev A, et al. Chemical inhibitor of nonapoptotic cell death with therapeutic potential for ischemic brain injury. Nat Chem Biol. 2005 Jul;1(2):112-9. doi: 10.1038/nchembio711. Epub 2005 May 29. Erratum in: Nat Chem Biol.
2005 Sep;1(4):234.
Ni H, Qin H, Sun C, et al. MiR-375 reduces the stemness of gastric cancer cells through triggering ferroptosis. Stem Cell Research & Therapy. 2021, 12(1): 1-17.
Zhang Y, Fan B Y, Pang Y L, et al. Neuroprotective effect of deferoxamine on erastininduced ferroptosis in primary cortical neurons. Neural Regeneration Research. 2020, 15(8): 1539
Yan B, Ai Y, Sun Q, et al. Membrane Damage during Ferroptosis Is Caused by Oxidation of Phospholipids Catalyzed by the Oxidoreductases POR and CYB5R1. Molecular Cell. 2020
hang C, Liu Z, Zhang Y, et al. Z"Iron free" zinc oxide nanoparticles with ion-leaking properties disrupt intracellular ROS and iron homeostasis to induce ferroptosis. Cell Death & Disease. 2020, 11(3): 1-15.
Yang K H, Tang J Y, Chen Y N, et al. Nepenthes Extract Induces Selective Killing, Necrosis, and Apoptosis in Oral Cancer Cells. Journal of Personalized Medicine. 2021, 11(9): 871.
D'Onofrio N, Martino E, Balestrieri A, et al. Diet-derived ergothioneine induces necroptosis in colorectal cancer cells by activating the SIRT3/MLKL pathway. FEBS letters. 2022
Wu H, Cheng X, Huang F, et al. Aprepitant Sensitizes Acute Myeloid Leukemia Cells to the Cytotoxic Effects of Cytosine Arabinoside in vitro and in vivo. Development and Therapy. 2020, 14: 2413
Wang Z, Zou F, Wang A, et al. Repurposing of the FGFR inhibitor AZD4547 as a potent inhibitor of necroptosis by selectively targeting RIPK1. Acta Pharmacologica Sinica. 2022: 1-10
Wang Y, Zhang B, Liu S, et al.The traditional herb Sargentodoxa cuneata alleviates DSS-induced colitis by attenuating epithelial barrier damage via blocking necroptotic signaling.Journal of Ethnopharmacology.2023: 117373.
Chen H, Hu J, Xiong X, et al.AURKA inhibition induces Ewing's sarcoma apoptosis and ferroptosis through NPM1/YAP1 axis.Cell Death & Disease.2024, 15(1): 99.
Wang X, Ji Y, Qi J, et al.Mitochondrial carrier 1 (MTCH1) governs ferroptosis by triggering the FoxO1-GPX4 axis- mediated retrograde signaling in cervical cancer cells.Cell Death & Disease.2023, 14(8): 1-13.
Shen B, et al. Necrostatin-1 Attenuates Renal Ischemia and Reperfusion Injury via Meditation of HIF-1α/mir- 26a/TRPC6/PARP1 Signaling. Mol Ther Nucleic Acids. 2019 Sep 6;17:701-713.
Li J, Liu X, Liu Y, et al.Saracatinib inhibits necroptosis and ameliorates psoriatic inflammation by targeting MLKL. Cell Death & Disease.2024, 15(2): 122.
Chen J, Liu Y, You Y, et al.Biotin-decorated celastrol-loaded ZIF-8 nanoparticles induce ferroptosis for colorectal cancer therapy.Materials & Design.2024: 112814.
Liao W, Zhang R, Chen G, et al.Berberine synergises with ferroptosis inducer sensitizing NSCLC to ferroptosis in p53-dependent SLC7A11-GPX4 pathway.Biomedicine & Pharmacotherapy.2024, 176: 116832.
Zheng M, Zhai Y, Yu Y, et al.TNF compromises intestinal bile-acid tolerance dictating colitis progression and limited infliximab response.Cell Metabolism.2024
Chen H, Hu J, Xiong X, et al.SETD8 inhibits apoptosis and ferroptosis of Ewing's sarcoma through YBX1/RAC3 axis. Cell Death & Disease.2024, 15(7): 494.
Hu Q, Chen Y, Zhang W, et al.Dehydroevodiamine targeting IKKβ to alleviate acute gastric injury via inhibiting the p65/NLRP3 axis.Phytomedicine.2024: 155963.
Xu C, Chen Y, Zhou Z, et al.ML385, an Nrf2 Inhibitor, Synergically Enhanced Celastrol Triggered Endoplasmic Reticulum Stress in Lung Cancer Cells.ACS Omega.2024
Zhang J, Gao Z, Yang Y, et al.SNF2L maintains glutathione homeostasis by initiating SLC7A11 transcription

through chromatin remodeling.Cell Death & Disease.2024, 15(11): 820.
Deng P, Silva M, Yang N, et al.Artemisinin inhibits neuronal ferroptosis in Alzheimer's disease models by targeting KEAP1.Acta Pharmacologica Sinica.2024: 1-12.
Ning X, Chen X, Li R, et al.Identification of a Novel Cuproptosis Inducer That Induces ER Stress and Oxidative Stress to Trigger Immunogenic Cell Death in Tumors.Free Radical Biology and Medicine.2025
Linkermann A, et al. The RIP1-kinase inhibitor necrostatin-1 prevents osmotic nephrosis and contrast-induced AKI in mice. J Am Soc Nephrol. 2013 Oct;24(10):1545-57.
Lei S, Chen C, Han F, et al.AMER1 deficiency promotes the distant metastasis of colorectal cancer by inhibiting SLC7A11-and FTL-mediated ferroptosis.Cell Reports.2023, 42(9).
Zhou Y, et al. Protective effects of necrostatin-1 against concanavalin A-induced acute hepatic injury in mice. Mediators Inflamm. 2013;2013:706156.
Zhou R, You Y, Zha Z, et al.Biotin decorated celastrol-loaded ZIF-8 nano-drug delivery system targeted epithelial ovarian cancer therapy.Biomedicine & Pharmacotherapy.2023, 167: 115573.
hang C, Liu Z, Zhang Y, et al. Z"Iron free" zinc oxide nanoparticles with ion-leaking properties disrupt intracellular ROS and iron homeostasis to induce ferroptosis[J]. Cell Death & Disease. 2020, 11(3): 1-15.
Zhu X, Huang N, Ji Y, et al.Brusatol induces ferroptosis in oesophageal squamous cell carcinoma by repressing GSH synthesis and increasing the labile iron pool via inhibition of the NRF2 pathway.Biomedicine & Pharmacotherapy.2023, 167: 115567.
Yao X, Ma S, Peng S, et al. Zwitterionic Polymer Coating of Sulfur Dioxide-Releasing Nanosystem Augments Tumor Accumulation and Treatment Efficacy[J]. Advanced Healthcare Materials. 2020, 9(5): 1901582.
Li H, Guan J, Chen J, et al.Necroptosis signaling and NLRP3 inflammasome cross-talking in epithelium facilitate Pseudomonas aeruginosa mediated lung injury.Biochimica et Biophysica Acta (BBA)-Molecular Basis of Disease. 2022: 166613.
Wu Z, Lin C, Zhang F, et al.TIGD1 Function as a Potential Cuproptosis Regulator Following a Novel Cuproptosis- Related Gene Risk Signature in Colorectal Cancer.Cancers.2023, 15(8): 2286.
Wang S, Li F, Qiao R, et al. Arginine-Rich Manganese Silicate Nanobubbles as a Ferroptosis-Inducing Agent for Tumor-Targeted Theranostics[J]. ACS nano. 2018 Dec 26;12(12):12380-12392.
Huang F, Liang J, Lin Y, et al.Repurposing of Ibrutinib and Quizartinib as potent inhibitors of necroptosis. Communications Biology.2023, 6(1): 972.